Arabidopsis TEBICHI, with Helicase and DNA Polymerase Domains, Is Required for Regulated Cell Division and Differentiation in Meristems [W][OA]

Soichi Inagaki,[a,1] Takamasa Suzuki,[a,2] Masa-aki Ohto,[b,3] Hiroko Urawa,[c,4] Takashi Horiuchi,[c] Kenzo Nakamura,[a] and Atsushi Morikami[d]

[a] Laboratory of Biochemistry, Graduate School of Bioagricultural Sciences, Nagoya University, Furo-cho, Chikusa, Nagoya 464-8601, Japan

[b] Division of Developmental Biology, National Institute for Basic Biology, Okazaki, Aichi 444-8585, Japan

[c] Division of Gene Expression and Regulation, National Institute for Basic Biology, Okazaki, Aichi 444-8585, Japan

[d] Department of Agrobiological Resources, Faculty of Agriculture, Meijo University, Tempaku, Nagoya 468-8502, Japan

In plant meristems, each cell divides and differentiates in a spatially and temporally regulated manner, and continuous organogenesis occurs using cells derived from the meristem. We report the identification of the *Arabidopsis thaliana TEBICHI* (*TEB*) gene, which is required for regulated cell division and differentiation in meristems. The *teb* mutants show morphological defects, such as short roots, serrated leaves, and fasciation, as well as defective patterns of cell division and differentiation in the meristem. The *TEB* gene encodes a homolog of *Drosophila* MUS308 and mammalian DNA polymerase θ, which prevent spontaneous or DNA damage–induced production of DNA double strand breaks. As expected from the function of animal homologs, *teb* mutants show constitutively activated DNA damage responses. Unlike other fasciation mutants with activated DNA damage responses, however, *teb* mutants do not activate transcriptionally silenced genes. *teb* shows an accumulation of cells expressing *cyclinB1;1:GUS* in meristems, suggesting that constitutively activated DNA damage responses in *teb* lead to a defect in G2/M cell cycle progression. Furthermore, other fasciation mutants, such as *fasciata2* and *tonsoku/mgoun3/ brushy1*, also show an accumulation of cells expressing *cyclinB1;1:GUS* in meristems. These results suggest that cell cycle progression at G2/M is important for the regulation of the pattern of cell division and of differentiation during plant development.

INTRODUCTION

The morphogenesis of higher plants depends on the activity of apical meristems, which develop during embryogenesis. Meristems consist of both slowly and rapidly dividing cells, and cells generated in the meristems differentiate according to their positional information. Although the meristem itself is highly stable and can function for prolonged periods, individual cells in the meristem change through division, expansion, and differentiation.

Therefore, there might be specific mechanisms that coordinate cell division and differentiation in the meristem.
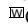
The intercellular communication mechanisms for controlling cell division and differentiation in the meristem are well studied in the model plant *Arabidopsis thaliana*. In the root apical meristem (RAM), quiescent center (QC) cells are surrounded by the initial cells for each cell lineage, and daughter cells generated from endodermis/cortex initial cells divide periclinally to form the endodermis and cortex cells. *SHORT-ROOT* (*SHR*) and *SCARE-CROW* (*SCR*) control this asymmetric cell division and the differentiation of endodermal cells (Scheres et al., 1995; Di Laurenzio et al., 1996; Helariutta et al., 2000). The SHR protein expressed in the stele moves into the neighboring endodermis, endodermis/cortex initials, and the QC. The translocated SHR induces the asymmetric cell division of endodermis/cortex initials by activating *SCR* and the differentiation of endodermis (Scheres et al., 1995; Nakajima et al., 2001). The shoot apical meristem (SAM) is organized into the central zone, which consists of lower organizing center cells and upper stem cells, and the peripheral zone, in which organ primordia develop. Stem cell fate and associated *CLAVATA3* (*CLV3*) gene expression are maintained by underlying organizing center cells expressing the *WUSCHEL* (*WUS*) gene (Laux et al., 1996; Mayer et al., 1998; Schoof et al., 2000). Conversely, *CLV3* restricts the size of the organizing center by repressing the expression of *WUS*, and *clv3*
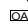
mutants show expansion of the SAM and the *WUS*-expressing region (Clark et al., 1995; Schoof et al., 2000).

Several genes regulating SAM size, organization, and stem cell identity have been identified in *Arabidopsis*. Loss-of-function mutations of *ULTRAPETALA1*, which encodes a putative transcriptional regulatory protein, result in enlargement of the SAM and expansion of the *WUS* expression domain, indicating that the ULTRAPETALA1 protein is a negative regulator of stem cell accumulation and size of the SAM (Fletcher, 2001; Carles et al., 2005). Furthermore, several groups recently reported that class III homeodomain–leucine zipper transcription factors, such as *CORONA*, *PHABULOSA*, *PHAVOLUTA*, and *REVOLUTA*, also regulate stem cell population and size of the SAM (Zhong and Ye, 2004; Green et al., 2005; Prigge et al., 2005; Williams et al., 2005). Also, the *mgoun1* (*mgo1*) and *mgo2* mutants show perturbed formation of organ primordia from the SAM as well as enlargement and disorganization of the SAM, suggesting that *MGO* genes control the step of cell fate determination required for the recruitment of cells from the peripheral zone to the organ primordia (Laufs et al., 1998). This observation proposes that smooth initiation and formation of organs from the meristem periphery is also required for the normal organization and size of the meristem itself.

Additional regulatory factors are emerging as important in the maintenance of the organization and size of the SAM. Mutants in which these factors are impaired are characterized by defects in the structure of both the SAM and the RAM. The *fasciata1* (*fas1*) and *fas2* mutants of *Arabidopsis* show stem fasciation, abnormal phyllotaxy, and short roots (Leyser and Furner, 1992). These phenotypes are attributable to a defect in meristem organization, and *fas* mutants are defective in the expression of *WUS* in the SAM and *SCR* in the RAM (Kaya et al., 2001). The *FAS1* and *FAS2* genes encode two subunits of the *Arabidopsis* counterpart of Chromatin Assembly Factor-1 (CAF-1) that are thought to be involved in chromatin assembly during DNA replication and repair. The FAS complex may control the state of gene expression by regulating the structure of chromatin (Kaya et al., 2001). The *TONSOKU* (*TSK*)/*MGO3* gene is also important for the maintenance of meristem structure, and a loss-of-function mutation in this gene disrupts the control of cell division and cellular arrangement in the SAM and the RAM (Guyomarc'h et al., 2004; Suzuki et al., 2004). The *tsk/mgo3* mutant shows altered expression of *WUS* in the SAM and *SCR* in the RAM as well as developmental phenotypes similar to those of the *fas* mutants, including short roots, abnormal phyllotaxy, and stem fasciation. Alleles of *tsk/mgo3* (*brushy1* [*bru1*]) have been isolated as mutants that show altered responses to DNA damage (Takeda et al., 2004). The *bru1* mutant shows hypersensitivity to several DNA-damaging agents and constitutively activates the expression of the DNA double strand break (DSB)–inducible gene, poly(ADP-ribose) polymerase-2 (At *PARP-2*). In addition, the *bru1* mutant shows stochastic release of transcriptional gene silencing (TGS). This release of TGS is also exhibited by *fas* mutants (Takeda et al., 2004). TSK/MGO3/BRU1 is a large protein containing LGN repeats and Leu-rich repeats, both of which are involved in protein–protein interactions (Guyomarc'h et al., 2004; Suzuki et al., 2004, 2005b; Takeda et al., 2004). The phenotypic similarities between *tsk/mgo3/bru1* and *fas* mutants suggest that the TSK/MGO3/

BRU1 protein is involved in the structural and functional maintenance of chromatin during DNA replication. In support of this notion, the tobacco (*Nicotiana tabacum*) homolog of the *TSK/MGO3/BRU1* gene is predominantly expressed at S-phase in synchronously cultured tobacco BY-2 cells (Suzuki et al., 2005a). Moreover, fasciated stems and release of TGS are found in mutants of *MRE11*, which is involved in the repair of DSBs, DNA damage–associated cell cycle checkpoint control, and telomere maintenance, as well as in mutants of the Structural Maintenance of Chromatin2 (SMC2) subunit of condensin, which is involved in chromosome condensation and cell cycle checkpoint control (Bundock and Hooykaas, 2002; Siddiqui et al., 2003; Takeda et al., 2004).

Here, we report the isolation and characterization of *Arabidopsis tebichi* (*teb*) mutants. The *teb* mutants have a disorganized pattern of cell division and differentiation in the apical meristems and during embryogenesis, and they show developmental defects similar to those of *tsk/mgo3/bru1* and *fas* mutants. The *TEB* gene encodes a homolog of *Drosophila* MUS308 and mammalian DNA polymerase θ (POLQ) that contains both helicase and DNA polymerase domains. Analysis of *teb* mutants suggests that normal cell cycle progression, especially in the G2/M-phase, is important for the patterning of cell division and differentiation in the plant meristem.

RESULTS

Mutation of *TEB* Affects Meristem Organization and Organ Morphology

While screening for mutants with short roots among independent lines in our original collection of T-DNA–mutagenized *Arabidopsis* plants (ecotype Columbia-0 [Col-0]), we identified a short-root mutant that exhibits phenotypes in the aerial part that are similar to those of the *tsk* mutant. We named this mutant *tebichi-1* (*teb-1*), which was taken from the word for the cloven hoof of a pig in the regional dialect of the southernmost area of Japan.

Ten days after germination, the roots of *teb-1* plants were approximately one-third as long as those from Col-0 plants (Figure 1A). This reduced growth became more pronounced at later time points. The seedlings produced their first root hair at a position closer to the root tip in *teb-1* than in Col-0 (Figures 1B and 1C), suggesting a smaller meristematic zone. In contrast with the well-organized cell alignment in the RAM of Col-0 (Figure 1D), the structure of the RAM in *teb-1* was disorganized, and individual cell types, such as QC or initial cells, were difficult to discern (Figure 1E).

The aerial part of *teb-1* plants also showed defects in morphology, such as abnormal phyllotaxy, highly serrated and asymmetric leaves (Figure 1G), and a fasciated stem (Figure 1I). The cellular organization of the SAM was severely disturbed in *teb-1* (Figures 1K and 1L; cf. Figure 1J). For example, the L1 and L2 layers of the SAM in the Col-0 plants mostly divided anticlinally and remained clonally distinct (Figure 1M), whereas they frequently showed irregular cell division in *teb-1* (Figure 1N). In summary, the SAM and RAM in the *teb* mutant show defects in the pattern of cell division and in overall structure, and the morphology of SAM- and RAM-derived organs such as leaves, stems, and roots was altered.
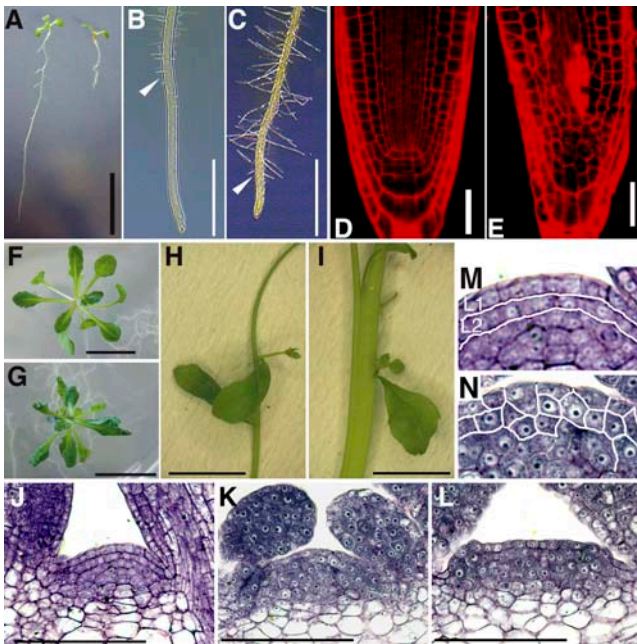
Figure 1. Developmental Phenotypes of the *teb* Mutant.

(A) Ten-day-old seedlings of wild-type Col-0 (left) and *teb-1* (right) plants. Bar = 2 cm.
(B) and **(C)** Root tips of Col-0 **(B)** and *teb-1* **(C)** plants. Arrowheads indicate the bottom of differentiated cells with root hairs. Bars = 2 mm.
(D) and **(E)** Propidium iodide–stained root tips of Col-0 **(D)** and *teb-1* **(E)** plants viewed by confocal laser scanning microscopy. Bars = 25 μm.
(F) and **(G)** Shoots of 20-d-old Col-0 **(F)** and *teb-1* **(G)** plants. Bars = 1 cm.
(H) and **(I)** Stem of Col-0 **(H)** and fasciated stem of *teb-1* **(I)**. Bars = 1 cm.
(J) to **(L)** Toluidine blue–stained sections of the SAM from 8-d-old Col-0 **(J)** and *teb-1* (**[K]** and **[L]**) plants. Bars = 100 μm.
(M) and **(N)** Higher magnification of the SAMs shown in **(J)** and **(K)**, respectively. L1 and L2 layers are indicated in Col-0 **(M)**, but the structure is disorganized in *teb-1* **(N)**.

The *teb* Mutant Shows an Irregular Pattern of Cell Division during Embryogenesis

Because *teb-1* has an aberrant pattern of cell division in post-embryonic development, we next examined whether it also shows a defective pattern of cell division during embryogenesis. The cell division pattern is strictly regulated during embryogenesis in *Arabidopsis* (Jurgens and Mayer, 1994). The zygote divides into an apical cell, which gives rise to the embryo, and a basal cell. The basal cell divides transversely to form the suspensor that connects the embryo to the seed tissue and an uppermost hypophysis that gives rise to the distal parts of the root meristem: the QC and columella root caps. Most embryos with the *teb-1* mutation showed normal development with a normal pattern of cell division until the 16-cell stage, although abnormal cell division occurred occasionally (Figure 2B). From the early globular stage, defects in the pattern of cell division became pronounced in *teb-1* embryos. In the early globular stage of the wild-type embryo, the hypophysis did not divide (Figure 2A). By contrast, early globular

embryos with the *teb-1* mutation often showed abnormal cell division, such as transverse division of the hypophysis and extra rounds of division of the suspensor cells (Figure 2C). In the wild type, outer cells in 16-cell embryos (protoderm) divided anticlinally to form the epidermis (Figures 2A, 2D, and 2G). By contrast, *teb-1* embryos often showed periclinal division of protoderm cells (arrowhead in Figure 2E). In severely affected *teb-1* embryos, there were many abnormal cell divisions and unusual cell expansions (Figure 2F). In the heart stage, most of the *teb-1* embryos showed an asymmetric and misshaped morphology as well as an aberrant cell division pattern, especially in the hypophysis descendents in the root pole (Figures 2H and 2I; cf. Figure 2G). In summary, *teb-1* showed an unusual pattern of cell division from early embryogenesis and produced morphologically abnormal embryos.

Altered Pattern of Cell Differentiation in the RAM of *teb* Mutants

To examine the effect of the *teb-1* mutation on cell differentiation, we analyzed the expression patterns of several cell type–specific markers in the root. Columella root cap cells specifically accumulate starch granules that are easily visualized by Lugol staining (Fukaki et al., 1998). Although the root cap of *teb-1* contained cells with starch granules, unlike the columella cells of Col-0 plants,
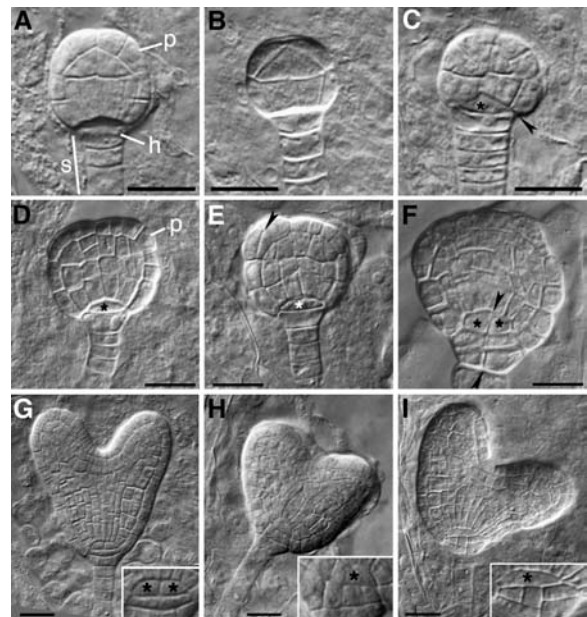
Figure 2. Embryo Phenotypes of the *teb* Mutant.

Developing embryos of Col-0 (**[A]**, **[D]**, and **[G]**) and *teb-1* (**[B]**, **[C]**, **[E]**, **[F]**, **[H]**, and **[I]**).
(A) to **(C)** Sixteen-cell to early globular stage embryos.
(D) to **(F)** Mid to late globular stage embryos.
(G) to **(I)** Heart stage embryos. Insets show magnified views of hypophysis cell descendants.
Arrowheads in **(C)**, **(E)**, and **(F)** indicate abnormal cell division in the *teb-1* embryo. Asterisks indicate lens-shaped cells or their descendents, which give rise to QC cells of the root. h, hypophysis; p, protoderm; s, suspensor. Bars = 25 μm.

they were not regularly organized (Figures 3A and 3B). Occasionally, we observed *teb-1* plants that had a split root tip (Figure 3C), which is a characteristic feature of the *tsk* mutant (Suzuki et al., 2004).

In Col-0 plants, expression of green fluorescent protein (GFP) under the control of the *SCR* promoter (*SCR*:*GFP*) Wysocka-Diller et al., 2000) was observed specifically in the QC and cortex/endodermis initials in the RAM, and its expression was continuous to the endodermis but not to the cortex (Figure 3D) (Helariutta et al., 2000). We introduced *SCR*:*GFP* into *teb-1* by a cross. Although *SCR*:*GFP* was expressed in some endodermal cells of roots in *teb-1*, its expression was not continuous and was largely missing in the endodermal cell layers (Figures 3E and 3F). In contrast with the *tsk* and *fas* mutants (Kaya et al., 2001; Suzuki et al., 2004), ectopic expression of *SCR*:*GFP* was not observed in *teb-1*. These results suggest that the normal expression of *SCR* in the endodermis is partially dependent on *TEB* gene function.

Auxin plays an important role in the function of the RAM, and its accumulation in columella initial cells is essential for the organization and maintenance of the cellular pattern of the RAM (Sabatini et al., 1999). To examine the distribution of auxin and the responsiveness to auxin in roots of *teb-1*, we analyzed the expression of a fusion of the β-glucuronidase (GUS; *uidA*) reporter gene and DR5, a synthetic auxin-responsive promoter (*DR5*:*GUS*) (Ulmasov et al., 1997). Similar to the Col-0 plant (Figure 3G) (Sabatini et al., 1999), maximal expression of *DR5*:*GUS* in the root tip of *teb-1* was observed around the columella initial cells (Figures 3H and 3I), although the expression pattern in some

Figure 3. Differentiation States in Roots of the *teb* Mutant.

(A) to **(C)** Lugol-stained root caps from Col-0 **(A)** and *teb-1* (**[B]** and **[C]**) plants. Starch granules in columella root caps were stained dark purple.
(D) to **(F)** *SCR*:*GFP* expression in root tips of Col-0 **(D)** and *teb-1* (**[E]** and **[F]**) plants.
(G) to **(I)** *DR5*:*GUS* expression in root tips of Col-0 **(G)** and *teb-1* (**[H]** and **[I]**) plants.
Bars = 50 μm.

teb-1 plants was slightly abnormal. These results suggest that the distribution of auxin and the responsiveness to auxin are essentially normal in the root tips of *teb-1* plants.

TEB Encodes a Protein with Helicase and DNA Polymerase I Domains

Genetic analysis of *teb-1* showed that phenotypes observed in *teb-1* were the result of a single recessive mutation not linked to T-DNA insertion (data not shown). To identify the gene for *teb*, we performed map-based cloning. Using a population of 1020 plants with the phenotypes conferred by *teb-1* in F2 progeny of crosses between *teb-1* and Landsberg *erecta*, we mapped the *teb-1* mutation to a 210-kb region between the F8B4a and T6I18a markers on the long arm of chromosome 4 (see Supplemental Figure 1 online). Because the frequency of recombination in this region was significantly lower than in other regions, we attempted to find a DNA fragment length polymorphism between Col-0 and *teb-1* using long-range PCR with the expectation that *teb-1* might be caused by the misintegration of T-DNA, which often accompanies deletion of the genome. As a result, we found a 2.7-kb deletion in the *teb-1* genomic DNA within the predicted protein-coding region At4g32700 (Figure 4A). The transcript of At4g32700 was confirmed by sequencing cDNA (accession number AV546006) in the cDNA library of the Kazusa DNA Research Institute. Nevertheless, further analysis of the transcribed region of this gene by RT-PCR and 5′ rapid amplification of cDNA ends PCR indicated that the transcript of this gene actually extends to the next predicted protein-coding region, At4g32695. Indeed, we could amplify a full-length cDNA of 6600 bp using a set of primers corresponding to the putative 5′ and 3′ untranslated regions of this gene (Figure 4C). The nucleotide sequence of this full-length cDNA confirmed the exon–intron organization of the *TEB* gene (Figure 4A). Among the collection of T-DNA insertion lines of the Salk Institute (Alonso et al., 2003), we identified two lines of plants that contain T-DNA integration in At4g32700 and At4g32695 (Figure 4A). Both of the T-DNA insertion lines had the same visible phenotypes as *teb-1* (Figures 4D and 4E), and allelism tests showed that these two lines and *teb-1* were allelic (see Supplemental Figure 2 online). These results confirmed that the *TEB* gene is covered by both At4g32700 and At4g32695. These T-DNA insertion lines are designated *teb-2* and *teb-5*.

The *TEB* gene consists of 28 exons and encodes a 2154–amino acid polypeptide. The TEB protein contains two conserved functional domains: an N-terminal superfamily II DNA/RNA helicase domain and a C-terminal prokaryotic-type DNA polymerase I domain (Figure 4A). The *TEB* gene is a single-copy gene, and no other gene in the *Arabidopsis* genome encodes a polypeptide with both of these domains. Homologs of the predicted TEB protein are found in multicellular eukaryotes, such as *Drosophila* MUS308 (Harris et al., 1996) and POLQ from mouse (Shima et al., 2003) and human (Seki et al., 2003) (Figure 4B). However, they are not found in bacteria or single-cell eukaryotes like yeast and fungi. Among the TEB homologs, amino acid sequences of the helicase and polymerase domains show a higher degree of conservation than the central region sequences (Figure 4B). The central regions of TEB and MUS308/POLQ of animals have no significant homology with other sequences.
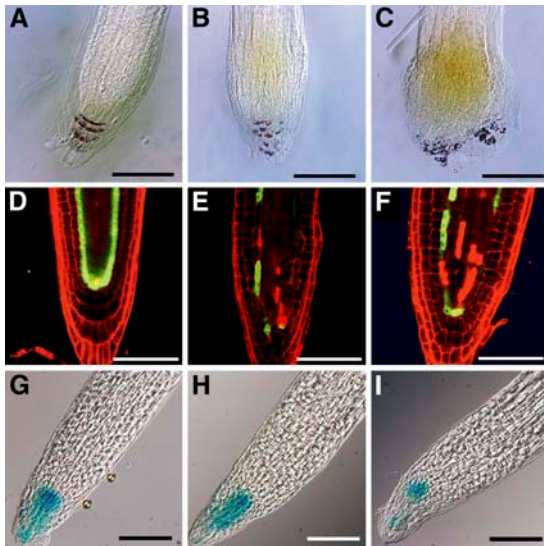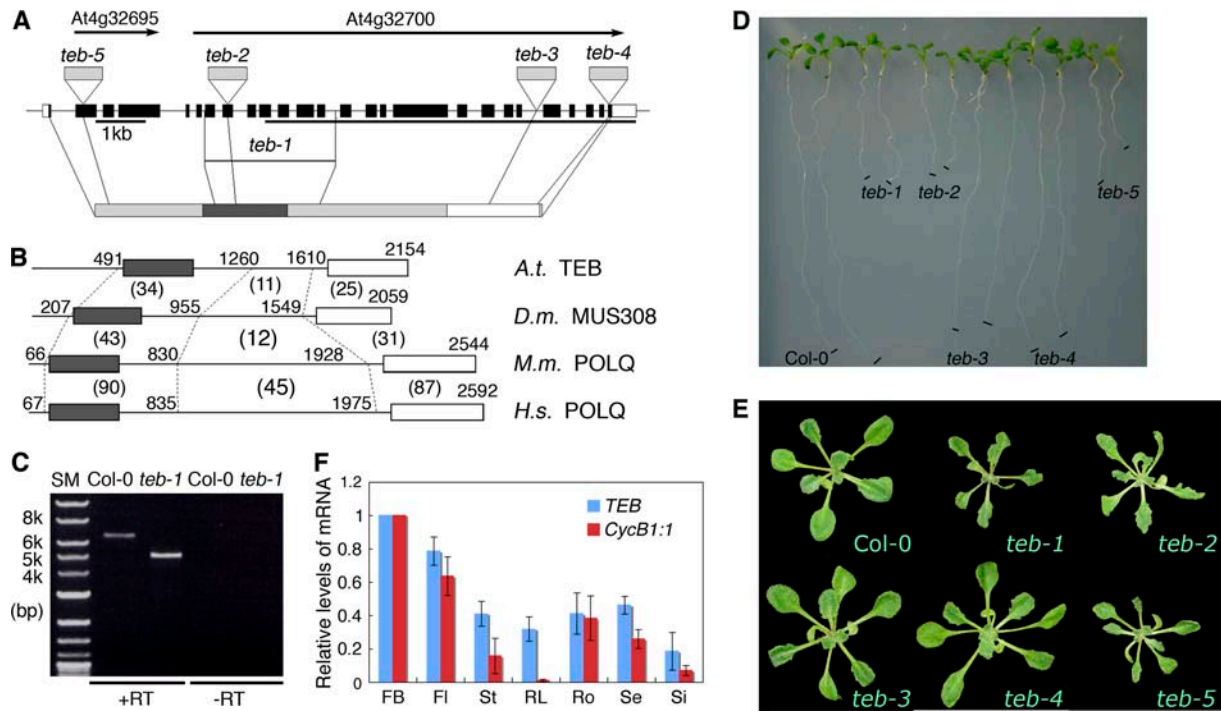
Figure 4. Molecular Characterization of the *TEB* Gene.

(A) Structure and mutant alleles of the *TEB* gene. Top, intron–exon structure of *TEB* and sites of mutation in the alleles. Rectangles represent exons. Black rectangles represent the coding region, and white rectangles represent 5′ and 3′ untranslated regions. Bottom, domain structure of the TEB protein. Predicted functional domains are indicated by dark gray boxes (helicase domain) and white boxes (DNA polymerase domain). The thick line below the intron–exon structure indicates the region covered by the cDNA clone in the cDNA library of the Kazusa DNA Research Institute.

(B) Structures of MUS308 and its homologs in higher eukaryotes. Dark gray rectangles represent helicase domains, and white rectangles represent DNA polymerase domains. Dotted lines separate the proteins into regions of highest conservation, with the least conserved region in the center and the N terminus. The percentage sequence identity between each pair is indicated in parentheses. *A.t.*, *Arabidopsis thaliana*; *D.m.*, *Drosophila melanogaster*; *M.m.*, *Mus musculus*; *H.s.*, *Homo sapiens*.

(C) RT-PCR analysis of *TEB* transcription in Col-0 and the *teb-1* mutant. At left, fragment lengths of the size marker (SM) are indicated. The negative control lacking reverse transcriptase is indicated by –RT, and the reactions containing reverse transcriptase are indicated by +RT.

(D) and **(E)** Morphological phenotypes in root **(D)** and shoot **(E)** of the alleles for *TEB*. The marks in **(D)** indicate the tips of the roots.

(F) Real-time RT-PCR analysis of *TEB* and *CycB1;1* gene expression in several organs. RNAs from flower buds (FB), flowers (Fl), stems (St), rosette leaves (RL), and roots (Ro) from 4-week-old Col-0 plants, 7-d-old seedlings (Se), and siliques (Si) were examined. Levels of 18S rRNA were used as a reference, and the values are expressed as ratios to the values in the flower buds. The values shown represent averages of three separate biological replicates ± SD.

The 2.7-kb deletion in *teb-1* eliminated the 7th through the 13th exons, which correspond to the helicase domain of the TEB protein (Figure 4A). This deletion did not abolish the expression of the mutated *TEB* gene but resulted in the production of a truncated transcript (Figure 4C). T-DNA insertions in *teb-2* and *teb-5* occurred in the second and eighth exons of the *TEB* gene, respectively (Figure 4A). We identified two additional T-DNA insertion lines, *teb-3* and *teb-4*, with insertions in the 21st intron and the last exon of *TEB*, respectively (Figure 4A). These have defects in the polymerase domain and the C terminus of the TEB protein, respectively, and the homozygous mutant plants exhibited phenotypes similar to that of Col-0 (Figures 4D and 4E). These results suggest that the developmental phenotypes of *teb* mutants are attributable to deficits in the helicase domain of the TEB protein.

We next examined the levels of *TEB* mRNA in various organs of Col-0 plants using quantitative real-time RT-PCR. The *TEB* gene was expressed in all of the organs examined, although its expression was highest in flower buds and flowers (Figure 4F). The flower buds and flowers contained the highest number of actively dividing cells, as indicated by the high expression of *CyclinB1;1* (*CycB1;1*) (Figure 4F). These results suggest that *TEB* functions in actively dividing cells, although *TEB* was also expressed in rosette leaves and stems, where expression of *CycB1;1* is very low (Figure 4F). Analysis of previously published microarray data for specific cell types from *Arabidopsis* root (Birnbaum et al., 2003) revealed that expression of the *TEB* gene is higher in the meristematic zone than in the more mature zone of the root.

teb Mutants Are Hypersensitive to DNA-Damaging Agents

TEB is a homolog of *Drosophila* MUS308 and mouse POLQ (Figure 4B). The defect in the *Drosophila* MUS308 gene causes

hypersensitivity to DNA cross-linking agents (Boyd et al., 1990; Leonhardt et al., 1993; Harris et al., 1996). The *chaos1* mouse mutant, which is deficient in POLQ, shows the accumulation of spontaneous and x-ray–induced DSBs (Shima et al., 2003). To examine the sensitivity of the *teb* mutants to DNA-damaging agents, we evaluated the effect of the DNA cross-linking agent mitomycin C (MMC) and the DNA-alkylating agent methyl-methane sulfonate (MMS) on the growth of *teb* mutant roots in a root-bending assay. Five-day-old seedlings grown on vertically oriented plates were transferred to fresh plates with medium containing various concentrations of DNA-damaging agents. The plates were then rotated orthogonally to observe the new growth of roots. The growth of *teb-1* roots in the presence of 0.2 mg/L MMC was approximately half of that on control medium without MMC, whereas the growth of Col-0 roots was not affected by MMC even at a concentration of 2 mg/L (Figure 5A). Similarly, *teb-1* was more sensitive to MMS than Col-0 (Figure 5B). These results show that *teb-1* is more sensitive than Col-0 to DNA-damaging agents. Notably, the growth of roots of the *teb-3*

mutant, which did not show obvious developmental defects, was slightly more sensitive to MMC than that of Col-0 plants (Figure 5A). The sensitivity of root growth to MMS was almost the same in the *teb-3* and Col-0 plants (Figure 5B).

We next examined the effect of long-term treatment with DNA-damaging agents on the growth and morphology of the *teb* mutants. Seven-day-old seedlings were transferred to fresh medium containing MMS and incubated for an additional 10 d. Although Col-0 plants grown on medium containing higher concentration of MMS were smaller, their morphology was not affected (Figure 5C). On the other hand, the growth of *teb-1* plants was severely affected by treatment with MMS (Figure 5C). Interestingly, the growth of *teb-3* plants, which exhibited wild-type phenotypes on the control medium, was also affected by MMS; they showed *teb-1*–like phenotypes, such as abnormal leaf shape, when treated with lower concentrations of MMS (Figure 5C). Similar results were obtained with MMC (data not shown). These results suggest that the developmental phenotypes of the *teb* mutants are connected to DNA damage responses.
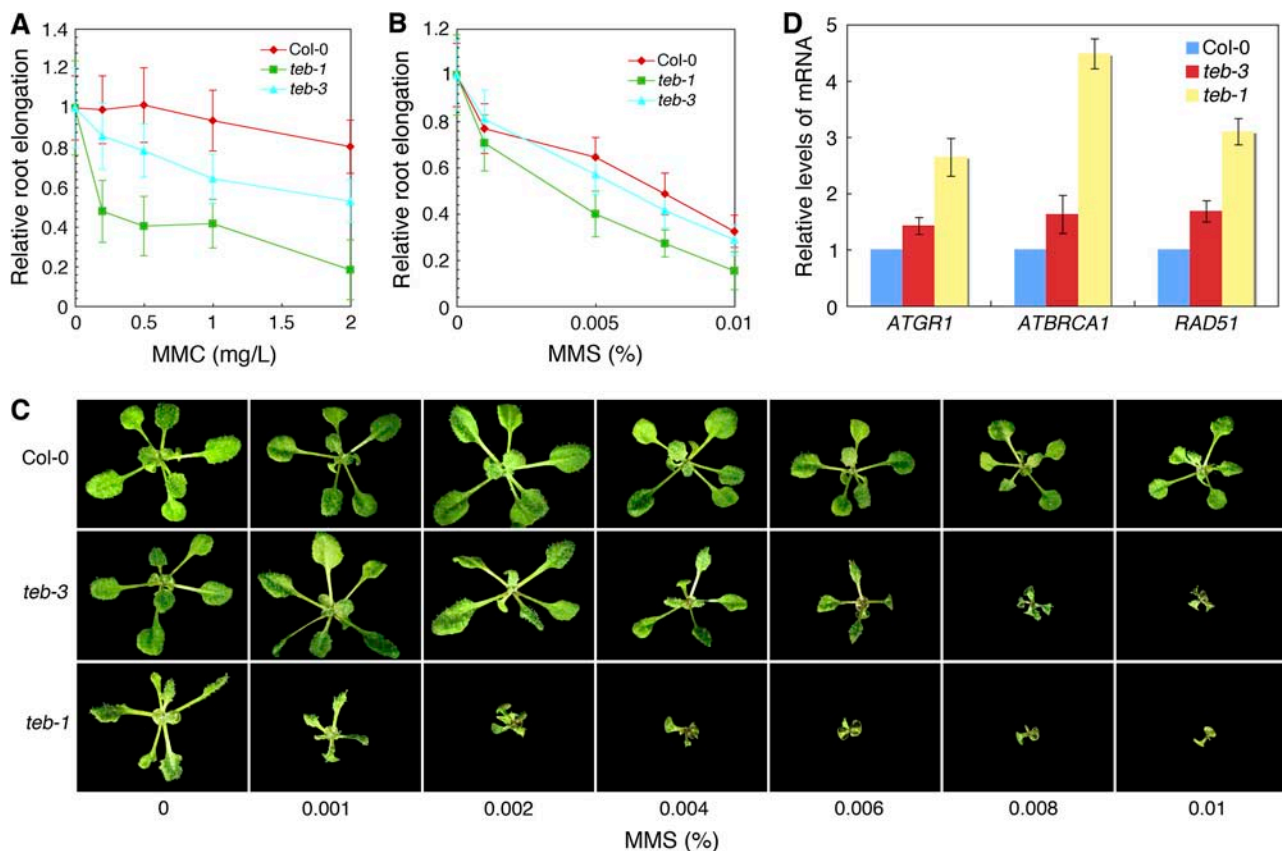

Figure 5. DNA Damage in *teb* Mutants.

(A) and **(B)** Sensitivity of root growth to the DNA-damaging agents MMC **(A)** and MMS **(B)**. Relative root elongation is the ratio of root elongation in medium containing the DNA-damaging agents to root elongation in control medium. Each point represents the average of the results from 40 to ~60 plants, and error bars represent SD.
(C) Shoot phenotypes of Col-0, *teb-1*, and *teb-3* on medium containing various concentrations of MMS.
(D) Real-time RT-PCR analysis of the expression of DSB-inducible genes in Col-0 and *teb* plants. The levels of 18S rRNA were used as a reference, and the values are expressed as ratios to the values in Col-0. The values shown represent averages of three separate biological replicates ± SD.

Constitutive Activation of DSB-Inducible Genes in *teb* Mutants

Because the *chaos1* mouse mutant has been reported to show chromosome fragmentation (Shima et al., 2003) and because the *mus308* mutant of *Drosophila* has an increased level of DSBs (Bilbao et al., 2002), we speculated that *teb* mutants also have an increased level of DSBs. To test this possibility, we examined the expression of DSB-inducible genes using real-time RT-PCR. The expression of *RAD51*, *GAMMA RESPONSE1* (*ATGR1*), and *BREAST CANCER SUSCEPTIBILITY1* (*ATBRCA1*) of *Arabidopsis* is strongly induced by γ irradiation (Klimyuk and Jones, 1997; Deveaux et al., 2000; Lafarge and Montane, 2003), and these genes are thought to function in the repair of damaged DNA or as part of the cell cycle checkpoint mechanism. As expected, *teb-1* showed 2.5- to 4.5-fold higher expression of these genes than Col-0 (Figure 5D). Although not as significant as that of *teb-1*, the expression of these genes was slightly higher in *teb-3* than in Col-0 (Figure 5D).

The *TEB* Gene Is Required for Efficient Intrachromosomal Recombination

Because *teb-1* showed constitutive activation of DSB-inducible genes and because DSBs are repaired in part by homologous recombination (Britt, 1999), we examined the effect of *teb-1* on the frequency of intrachromosomal homologous recombination. To assess the frequency of intrachromosomal homologous recombination, we used a transgenic line with a T-DNA containing the recombination substrate, in which two 3′ and 5′ deleted GUS genes with partially overlapping sequences are separated by a hygromycin resistance gene (Figure 6A) (Urawa et al., 2001). Reconstitution of a functional GUS gene by homologous recombination can be detected as a blue spot or sector upon histochemical GUS staining. The T-DNA also contains a non-transcribed spacer (NTS) between rRNA genes of *Arabidopsis*. The NTS in *Saccharomyces cerevisiae* covers a DNA element that enhances mitotic recombination in nearby regions (Keil and Roeder, 1984), and studies using these recombination substrate lines previously showed that the NTS sequence of *Arabidopsis* activates recombination events (Urawa et al., 2001). We crossed the recombination substrate lines F25 and F40 (Urawa et al., 2001) with the *teb-1* mutant. We obtained an F2 population with the recombination substrate transgene, which segregated into normal and *teb*-like phenotypes, and used it to compare the frequency of homologous recombination between the wild type and *teb-1*. Three-week-old plants with at least one copy of the recombination substrate were selected by PCR amplification of part of the GUS gene, and wild-type (*TEB/TEB* and *TEB/teb-1*) and *teb-1* (*teb-1/teb-1*) plants, identified by their morphological phenotypes, were stained for GUS activity. Despite the constitutive activation of DSB-inducible genes in *teb-1*, the number of GUS spots in individual *teb-1* plants apparently decreased and the average number per plant was twofold to fourfold lower in *teb-1* than in the wild type (Figure 6B). This finding suggests that TEB is involved in a process of intrachromosomal homologous recombination that is likely activated by NTS.
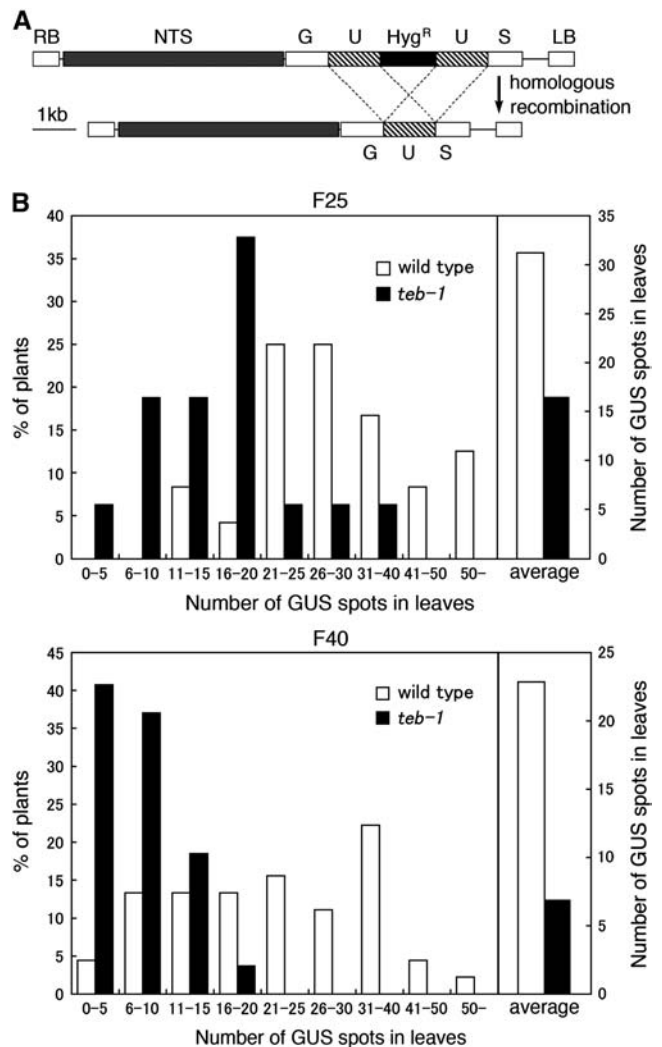

Figure 6. Intrachromosomal Recombination in the *teb-1* Mutant.

(A) Structure of T-DNA pBI-F used to monitor homologous recombination events (Urawa et al., 2001). The top diagram shows the structure of the T-DNA region in pBI-F, and the bottom diagram shows the intact GUS gene reconstituted by intrachromosomal homologous recombination. Hyg^R, hygromycin resistance gene; LB, left border; RB, right border.
(B) Homologous recombination frequency determined by histochemical staining of leaves from 3-week-old plants. The graphs at left show the distribution of plants with the indicated number of GUS spots on leaves, and the graphs at right show the average number of GUS spots per individual plant. Two individual transgenic lines, F25 and F40, were tested in the wild-type backgrounds (*TEB/TEB* and *TEB/teb-1*) and the *teb-1* background (*teb-1/teb-1*).

Release of TGS Does Not Occur in *teb* Mutants

Takeda et al. (2004) previously reported that release of silencing of transcriptionally silent information (TSI) occurs in a number of fasciated mutants, such as *fas* (Kaya et al., 2001), *bru1* (*tsk/mgo3*) (Takeda et al., 2004), and *mre11* (Bundock and Hooykaas, 2002), as well as in a mutant of the SMC2 subunit of condensin (Siddiqui et al., 2003). TSI comprises a specific class of pericentromeric

repeats and was identified as an endogenous target of TGS in *Arabidopsis* (Steimer et al., 2000). Expression from the TSI locus is transcriptionally repressed in the wild type, whereas it is activated in mutants with defects in the maintenance of TGS (Steimer et al., 2000; Saze et al., 2003). This suggests a possible link between the instability of epigenetic states in heterochromatin and the disorganization of meristem structure.

To determine whether *teb* mutants have altered epigenetic regulation of heterochromatin, we examined their expression of TSI repeats. RT-PCR (Figure 7) and RNA gel blot hybridization (data not shown) showed that the expression of TSI transcripts in *teb-1* and *teb-3* was not significantly different from that in Col-0 (Figure 7). By contrast, expression of the TSI transcripts was increased in the *fas1-1* mutant, as reported previously (Figure 7) (Takeda et al., 2004). These results indicate that *teb* mutants do not have altered epigenetic regulation of heterochromatin, at least with respect to the release of TSI repeats.

The *teb* Mutant Is Defective in G2/M Progression

Because the expression of cell cycle checkpoint–related genes is constitutively activated in *teb-1*, we speculated that *teb-1* might have a defect in cell cycle progression at a specific phase. Therefore, we examined the mitotic index in the RAM of *teb-1*. There were fewer mitotic figures (metaphase, anaphase, and telophase) in the RAM of *teb-1* than in Col-0 plants (Figure 8A), suggesting that *teb-1* has a defect in the entry into M-phase. Next, we crossed *teb-1* with a transgenic line harboring *CycB1;1:GUS* (Colon-Carmona et al., 1999), which consists of the *Arabidopsis CycB1;1* promoter driving a fusion of the CycB1;1 mitotic destruction box and GUS (cyclin-GUS). The *CycB1;1* promoter is activated in G2-phase, and the accumulated cyclin-GUS proteins are degraded by the anaphase-promoting complex at metaphase. The number of cells expressing cyclin-GUS in the RAM of *teb-1* was dramatically higher than in Col-0 (Figures 8B and 8C). Within the shoot, there were more cells expressing cyclin-GUS in the shoot apices of *teb-1* than in Col-0 (Figures 8F, 8G, 8J, and 8K). In *teb-1*, cells expressing cyclin-GUS were present in the more mature distal zone of leaves, whereas in
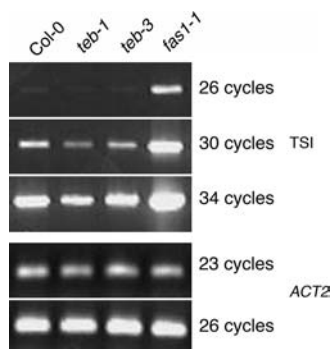

Figure 7. TGS in *teb* Mutants.

Semiquantitative RT-PCR analysis of TSI expression in the *teb-1* and *teb-3* mutants. Expression of TSI in Col-0 and *fas1-1* plants was measured as negative and positive controls, respectively. Expression of the *ACTIN2* gene was used as a reference.

Col-0, they were restricted to the proximal region of young leaves (cf. Figures 8F and 8G). Furthermore, the intensity of GUS staining in each GUS-expressing cell in the SAM was stronger in *teb-1* than in Col-0 (Figures 8J and 8K). These results suggest that the G2-to-M progression is retarded and that the extended G2-phase causes the accumulation of cyclin-GUS in cells of *teb-1*.

To further analyze the defect of cell cycle progression in *teb-1*, we used RT-PCR to examine the expression of *CycB1;1* and other cell cycle–regulated genes in shoot apices and young leaves of Col-0 and *teb-1* seedlings. Consistent with the observations in *CycB1;1:GUS* transgenic plants, we found that the level of the *CycB1;1* transcript was approximately threefold higher in *teb-1* than in Col-0 (Figure 8N). The level of transcript for *WEE1*, which is a cyclin-dependent kinase (CDK)–inhibitory kinase (Sorrell et al., 2002), was also higher in *teb-1* than in Col-0 (Figure 8N). We also examined the expression of the plant-specific CDK, CDKB, whose expression is strictly regulated during the cell cycle and is activated between S- and M-phases. There was an increase in the level of *CDKB1;1* mRNA in *teb-1*, whereas the level of *CDKB2;1* mRNA did not differ between Col-0 and *teb-1* (Figure 8N). Whereas CDKB1 is expressed from S- to early M-phase, CDKB2 is expressed in the more restricted phase of G2/M (Segers et al., 1996; Umeda et al., 1999; Menges et al., 2002). These results support the idea that the G2-to-M progression of the cell cycle is retarded in *teb-1*.

The *fas2* and *tsk/mgo3/bru1* Mutants Are Also Defective in G2/M Progression

Similar to the *teb-1* mutant, we recently reported that the *tsk-3* mutant shows an accumulation of cyclin-GUS–expressing cells in the RAM (Suzuki et al., 2005a). Because the *teb*, *tsk/mgo3/bru1*, and *fas* mutants share similar phenotypes, including hypersensitivity to DNA-damaging agents and defective meristem structure with fasciated stems and short roots (Leyser and Furner, 1992; Kaya et al., 2001; Suzuki et al., 2004; Takeda et al., 2004), it seemed likely that the *fas* mutant also shows defective cell cycle progression. We found that cells expressing cyclin-GUS accumulated in the root tips (cf. Figures 8D and 8E) and shoot apices (Figures 8H and 8L) of *fas2-2* plants as well as in the shoot apices of *tsk-3* (Figures 8I and 8M). Compared with *teb-1* and *fas2-2*, *tsk-3*, which shows more severe disorganization of the SAM, had increased levels of cyclin-GUS in the SAM (cf. Figure 8M with Figures 8K and 8L), supporting the idea that disorganization of the meristem structure is connected to the defect in G2/M progression.

DISCUSSION

In this study, we show that the novel *TEB* gene is required for the maintenance of structure of the SAM and the RAM as well as for cell cycle progression. Phenotypes similar to that of the *teb* mutants have been observed in mutants that are defective in genome maintenance, including DNA replication, DNA repair, and the DNA damage–associated cell cycle checkpoint, such as *fas* for CAF-1 (Kaya et al., 2001), *mre11* (Bundock and Hooykaas, 2002), and *tsk/mgo3/bru1* (Guyomarc'h et al., 2004; Suzuki et al., 2004; Takeda et al., 2004). Their phenotypes, however, vary in severity, frequency, and organs that most frequently show
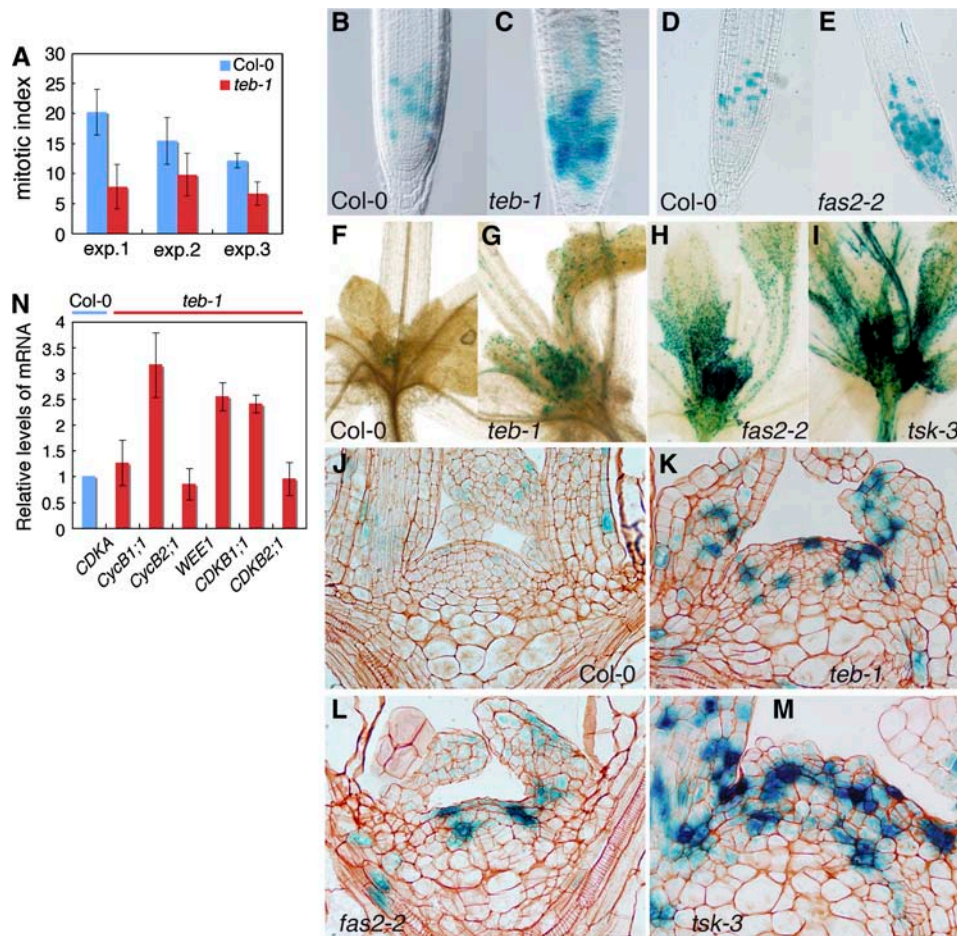
Figure 8. Defective Cell Cycle Progression in the *teb*, *tsk/mgo3/bru1*, and *fas2* Mutants.

(A) Mitotic index in the RAM of 5-d-old Col-0 and *teb-1* seedlings. The mitotic index is the number of mitotic figures (metaphase, anaphase, and telophase cells) within 150 μm of the QC cells. The cortex and endodermis cell layer in one section of this region contains ∼80 cells in both Col-0 and *teb-1* plants. Approximately 10 plants for each line were tested in one experiment. Error bars represent SD.

(B) to **(M)** Expression of cyclin-GUS in the RAM (**[B]** to **[E]**), young leaves (**[F]** to **[I]**), and the SAM (**[J]** to **[M]**) of Col-0 (**[B]**, **[D]**, **[F]**, and **[J]**), *teb-1* (**[C]**, **[G]**, and **[K]**), *fas2-2* (**[E]**, **[H]**, and **[L]**), and *tsk-3* (**[I]** and **[M]**) plants. Tissues from plants of the following ages were analyzed: RAM, 5 d old; young leaves, 14 d old; SAM, 7 d old.

(N) Real-time RT-PCR analysis of levels of mRNAs for cell cycle–regulated genes in Col-0 and *teb-1* plants. The levels of 18S rRNA were used as a reference, and the values are expressed as ratios to the values in Col-0. The values shown represent averages of three separate biological replicates ± SD.

morphological defects. The morphology of the *teb* mutants is similar to that of *tsk*, especially with respect to cell arrangement and differentiation in the RAM. In particular, both *teb* and *tsk* mutants occasionally show split root tips (Suzuki et al., 2004). Analysis of these mutants is expected to elucidate the mechanism that limits the stem cell niche of the meristem (e.g., the QC in the RAM).

Genome Maintenance Is Defective in *teb* Mutants

Higher levels of *ATGR1*, *ATBRCA1*, and *RAD51* were expressed in *teb-1* than in Col-0. Expression of these genes is induced in response to the accumulation of DNA damage, such as DSBs after γ irradiation, and these genes are thought to be involved in DNA repair or cell cycle checkpoints (Klimyuk and Jones, 1997; Deveaux et al., 2000; Lafarge and Montane, 2003). It has been

suggested that the *teb* mutation causes constitutive activation of the DNA repair and cell cycle checkpoint pathways. In addition, we show here that cell cycle progression at the G2/M-phase is affected in *teb-1*. CAF-1 facilitates the incorporation of histones H3 and H4 into newly synthesized DNA during S-phase (Smith and Stillman, 1989). In human cells, dominant-negative mutation of the CAF-1 p150 subunit results in stalled replication forks that are inappropriately processed and leads to the accumulation of DSBs and activation of the cell cycle checkpoint (Ye et al., 2003). In *Xenopus*, depletion of MRE11 leads to the spontaneous accumulation of DSBs during DNA replication (Costanzo et al., 2001). Furthermore, the *bru1* (*tsk/mgo3*) mutant shows constitutive expression of the DNA damage–inducible At *PARP-2* gene (Takeda et al., 2004). We found that *fas2* and *tsk/mgo3/bru1* as well as the *teb* mutants accumulate cells in the G2/M-phase in

meristems (Suzuki et al., 2005a). These observations suggest that constitutive activation of DNA damage responses is a common feature of the *teb*, *tsk/mgo3/bru1*, *fas*, and *mre11* mutants.

The ataxia–telangiectasia-mutated (ATM) and related ATM and Rad3-related (ATR) pathways, which regulate the cell cycle checkpoint, DNA repair, and apoptosis, are well studied in animals (for reviews, see Abraham, 2001; Shiloh, 2003). The ATM kinase is activated by DNA damage, such as DSBs, and activates downstream signaling pathways, leading to transient arrest of the cell cycle, inhibition of DNA replication, repair of DNA, and apoptosis. On the other hand, the ATR kinase is activated by stalled replication forks, which can occur spontaneously or after genotoxic stress, including UV light or hydroxyurea, and it regulates the slowing of the cell cycle during S-phase and G2/M progression (Abraham, 2001). In *Arabidopsis*, ATM and ATR homologs are important in the cellular response to DSBs and replication abnormalities, respectively, suggesting that similar systems regulating the cell cycle checkpoint exist in plants (Garcia et al., 2003; Culligan et al., 2004). DSB-induced expression of *ATGR1* and *RAD51* is dependent on the ATM kinase (Garcia et al., 2003), and activation of the expression of these two genes is greatly reduced in the *teb atm* double mutant (S. Inagaki, K. Nakamura, and A. Morikami, unpublished data), suggesting that the ATM-dependent checkpoint is activated in the *teb* mutant. At the same time, it is also possible that the ATR-dependent pathway associated with DNA replication abnormality is activated in *teb*. It was recently reported that treatment of *Arabidopsis* plants with the DNA replication inhibitor aphidicolin leads to the accumulation of cells expressing cyclin-GUS in the RAM, whereas this response is not found in a disruptant of the *ATR* gene (Culligan et al., 2004), suggesting that inhibition of DNA replication leads to the activation of the ATR-dependent checkpoint and the arrest of cell cycle progression at G2/M. Thus, it is possible that some aspects of the phenotypes conferred by *teb-1* are related to abnormal DNA replication. Detailed analysis of the genetic interaction between *teb* and other fasciation mutants, and mutants of the *ATM* and *ATR* genes, may help clarify the connection between the response to DNA damage and meristem maintenance.

NTS-activated intrachromosomal homologous recombination in *teb-1* seemed to be less frequent than in Col-0 (Figure 6). In *S. cerevisiae*, recombination hotspots have been found in the NTS between rRNA genes, which contain replication fork–blocking sites, including the replication fork barrier (Brewer and Fangman, 1987; Kobayashi et al., 1992). In addition, in *Arabidopsis*, the NTS sequence has been shown to activate homologous recombination in nearby chromosomal regions (Urawa et al., 2001). Replication blockage by the replication fork barrier or by DNA damage is overcome by homologous recombination (reviewed in Barbour and Xiao, 2003). The *teb* mutant may be defective in this mechanism to avert replication blockage, which could then cause a defect in the completion of DNA replication that would induce DNA damage.

TEB Is a Homolog of MUS308/POLQ That Contains Helicase and Polymerase Domains

The *TEB* gene encodes a homolog of *Drosophila* MUS308 and mammalian POLQ proteins. Unlike the *teb* mutants, the *mus308*

mutant of *Drosophila* and the *chaos1* mutant of mouse, which have defective *Polq* genes, do not show developmental defects under normal growth conditions (Leonhardt et al., 1993; Shima et al., 2003). Thus, the TEB protein may be involved in some plant-specific functions that are distinct from the functions of MUS308/POLQ in animals, even though these proteins have common functions, at least in genome maintenance.

TEB and MUS308/POLQ proteins have two characteristic conserved functional domains that are likely to be involved in DNA metabolism: an N-terminal helicase domain and a C-terminal DNA polymerase I domain. The N-terminal helicase domains of TEB and MUS308/POLQ contain seven motifs, including a DEXH box, that are characteristic of most superfamily II DNA and RNA helicases, and some of the residues within these motifs are specific to the TEB/MUS308/POLQ helicases (Harris et al., 1996; Tuteja and Tuteja, 2004). These residues may confer functional specificity to this particular class of helicases. The C-terminal polymerase domains of TEB and MUS308/POLQ belong to the PolA family DNA polymerases, which are related to *Escherichia coli* DNA polymerase I (Harris et al., 1996; Seki et al., 2003; Shima et al., 2003). DNA polymerase ν (POLN) is another PolA family DNA polymerase related to POLQ found in human and mouse (Marini et al., 2003); however, *Drosophila* and *Arabidopsis* lack proteins that are homologous with POLN, suggesting that the functions mediated by TEB cannot be performed by other proteins.

Fractionation of DNA polymerase activities from *Drosophila* embryos has revealed that *mus308* embryos are missing a peak of activity with an estimated molecular mass of 200 to 300 kD, suggesting that the activity is attributable to the MUS308 protein (Oshige et al., 1999). Expression of human POLQ in a baculovirus system showed that it has DNA polymerase and single-stranded DNA-dependent ATPase activities but lacks helicase activity (Seki et al., 2003). Also, helicase activity has not been reported for MUS308/POLQ family proteins.

Unlike *teb-1*, *teb-2*, and *teb-5*, which have disruptions of the N-terminal portion of the *TEB* gene, defects in the C-terminal DNA polymerase domain of TEB in *teb-3* and *teb-4* did not affect morphology under normal conditions; however, *teb-3* showed increased sensitivity to MMC and exhibited a morphological phenotype similar to that of *teb-1* when treated with DNA-damaging agents. Thus, the helicase and DNA polymerase domains may work together during morphogenesis and the cellular response to DNA damage, whereas the helicase domain alone may be sufficient to fulfill its function under normal conditions. Alternatively, the helicase but not the DNA polymerase domain of TEB may participate in the DNA damage response and morphogenesis, whereas the C-terminal part of TEB may influence the structure or stability of the helicase domain.

TGS Is Not Affected by the *teb* Mutation

As described above, common phenotypes attributable to meristem disorganization were found in the *teb*, *tsk/mgo3/bru1*, *fas*, and *mre11* mutants as well as in plants containing a disruption of the SMC2 subunit of condensin. One explanation for this is that the defect in epigenetic control could lead to the dysregulated expression of genes related to meristem organization. For

example, the *fas* mutants ectopically express *WUS* and *SCR* (Kaya et al., 2001), and yeast cells deficient in CAF-1 release the repression of gene expression at telomeres and mating-type loci (Monson et al., 1997; Enomoto and Berman, 1998; Zhang et al., 2000). Condensin could also be involved in the epigenetic regulation of gene expression. One of the regulatory proteins of the *Drosophila* condensin subunit interacts with Polycomb group proteins to maintain the transcriptional silencing of homeotic genes (Lupo et al., 2001). Takeda et al. (2004) reported that derepression of the transcriptional silencing of the TSI locus occurs in *fas*, *bru1* (*tsk/mgo3*), and *mre11* mutants as well as in the disruptant of SMC2. However, we did not observe the activation of TSI in *teb* mutants. Similarly, the *mus308* mutant of *Drosophila* did not display developmental defects reminiscent of a disruption in the epigenetic regulation of homeotic genes (Leonhardt et al., 1993). These results suggest that a defect in epigenetic regulation alone may not explain the phenotypes of these fasciation mutants.

Function of *TEB* in Cell Cycle and Differentiation

The *teb* mutant showed a partial loss of *SCR:GFP* expression in endodermal cells and QC cells in the root tip. Several possible mechanisms can explain how a defect in cell cycle progression leads to a defect in cell differentiation. First, it is possible that stochastic delay of cell cycle progression in the meristem causes improper cell organization, which in turn affects the positional information essential for proper cell differentiation. In *Arabidopsis* embryos, the pattern of cell division (rate, sequence, and orientation of division) is strictly regulated (Jurgens and Mayer, 1994), and manipulation of the cell cycle by downregulating *cyclinA3;2* has been shown to affect pattern formation in the embryo (Yu et al., 2003), suggesting that regulation of cell cycle progression is required for the regular pattern of cell division and, eventually, for the normal development of the embryo. Indeed, *teb* mutants frequently showed irregular patterns of cell division starting from early embryogenesis. The pattern of cell division is also important for regular cellular organization in postembryonic development. For example, cortex/endodermis initial cells in the RAM divide anticlinally, and their daughter cells divide periclinally to generate the cortex and endodermal cells (Scheres et al., 1994). These concerted cell divisions and the process of cell fate decision could be altered in *teb* mutants, resulting in disruption of the cell differentiation program. While this article was being prepared, Jenik et al. (2005) reported that a mutation in DNA polymerase ε (*tilted1-4*) causes a lengthening of the cell cycle as well as a disruption of the pattern of cell division, which results in the perturbation of cell fate specification in the hypophyseal lineage of the *Arabidopsis* embryo.

A second possible explanation for how a defect in cell cycle progression leads to a defect in cell differentiation is that progression through a specific phase of the cell cycle may be required for proper gene expression during cell fate decision. Some examples of this mechanism have been reported in animals. For example, expression of the *Drosophila even-skipped* gene, which specifies neurons, depends on progression through the S-phase of the cell cycle. Progression through the S-phase temporarily leads to the removal of chromatin-remodeling fac-

tors from chromatin, inhibiting the expression of the *even-skipped* gene (Weigmann and Lehner, 1995). It is possible that a delay in a specific phase of the cell cycle in the *teb* mutants affects the activation of some factors, such as *SCR*, that are involved in asymmetric cell division and cell differentiation.

METHODS

Plant Materials and Growth Conditions

The *teb-1* mutant of *Arabidopsis thaliana* was identified among T-DNA insertion lines generated by our group, whereas the other *teb* mutants, including SALK_035610 (*teb-2*), SALK_001669 (*teb-3*), SALK_037552 (*teb-4*), and SALK_018851 (*teb-5*), were obtained from the ABRC. The *fas1-1* (ecotype Enkheim) mutant and *fas2-2* (ecotype Nossen), which was crossed four times to Col-0, were kind gifts of T. Araki and H. Kaya of the Graduate School of Science, Kyoto University.

Plants were grown on MS medium (Murashige and Skoog, 1962) containing 2% sucrose and buffered with 2-morpholino ethanesulfonic acid monohydrate–KOH, pH 5.7. For observation of roots, the medium was solidified with 1.5% agar, and for observation of aerial parts, the medium was solidified with 0.3% gellan gum. All plants were grown under continuous light (65 μmol·m^{-2}·s^{-1}) at 22°C.

Observation of Plant Morphology and Gene Expression

Propidium iodide staining and fluorescence of GFP expression were observed using confocal laser scanning microscopy (FV500; Olympus), as described by Helariutta et al. (2000). To observe developing embryos, whole developing seeds were cleared in 8:1:2 (w/v/v) chloral hydrate:glycerol:water, and embryos were visualized using Nomarski optics on an Olympus BX60 microscope. Lugol staining of roots was performed as described by Fukaki et al. (1998). To visualize nuclei in roots and to count mitotic figures, propidium iodide staining was performed as described by Boisnard-Lorig et al. (2001). Histochemical staining of GUS activity was performed as described by Donnelly et al. (1999). For sections, tissues were fixed in 1:1:18 formalin:acetic acid:70% ethanol, dehydrated in a graded series of ethanol, and embedded in Technovit 7100 resin (Heraeus Kulzer) according to the manufacturer's instructions. Sections (3 to 5 μm thick) were stained with 0.05% toluidine blue or 0.01% aqueous safranin.

Map-Based Cloning of the *TEB* Gene

The *teb-1* mutant was crossed with Landsberg *erecta* wild-type plants. DNA samples from 1020 F2 plants were analyzed using simple sequence length polymorphism and cleaved-amplified polymorphic sequence markers (for details, see Supplemental Table 1 online), which were generated based on polymorphism data provided by Cereon (http://www.Arabidopsis.org/Cereon). Long-range PCR was performed using Herculase hotstart DNA polymerase (Stratagene) and primers designed to amplify 23 10-kb fragments covering a 210-kb region of the genome that includes the *teb* mutation site. RT-PCR for full-length cDNA was performed using Super-Script III reverse transcriptase (Invitrogen), Platinum Taq DNA polymerase high fidelity (Invitrogen), and primers designed to hybridize to predicted 5′ and 3′ untranslated regions of the *TEB* gene.

Real Time RT-PCR

Expression of the *TEB* gene, DSB-inducible genes, and cell cycle–regulated genes was analyzed by quantitative real-time RT-PCR using an iCycler iQ (Bio-Rad) with iQ SYBR Green Supermix (Bio-Rad). The cDNA strand synthesized from DNase-I–treated mRNA using oligo(dT)

primer was used as a template. Primer pairs for each gene were designed to amplify specific fragments of ∼100 bp. The primer sequences were as follows: 5′-CGATGATAGCTGCAAAATGGACTGG-3′ (forward) and 5′-GCACCCATTCCATAAAGAATTCCGTAG-3′ (reverse) for *TEB*; 5′-CCA-TGTATTTTGCAATGCGTG-3′ (forward) and 5′-TGTGGAGCACCTCGAA-TCTCT-3′ (reverse) for *ATBRCA1*; 5′-CGAGGAAGGATCTCTTGCAG-3′ (forward) and 5′-GCACTAGTGAACCCCAGAGG-3′ (reverse) for *RAD51*; 5′-GAAGGAGCAGACAAAGTGAG-3′ (forward) and 5′-GGTGAGATG-GAAGTGATAGG-3′ (reverse) for *ATGR1*; 5′-CTGAGTTCGTTTCCTACT-TATATTC-3′ (forward) and 5′-GATACAAGAAACTGATCTCAAAAGC-3′ (reverse) for *CDKA1*; 5′-TAAGCAGATTCAGTTCCGGTCAAC-3′ (forward) and 5′-GGGAGCTTTACGAAAGAAATACTCC-3′ (reverse) for *CycB1;1*; 5′-TTGGACAAAAGCTTACCAGTAGAAG-3′ (forward) and 5′-AGAGA-AGATATCGACTTTATCAAGG-3′ (reverse) for *WEE1*; 5′-GAAGTTCATTG-CTGTATCTGTTGTC-3′ (forward) and 5′-CCAAACATAAGACACTAATG-TGTCG-3′ (reverse) for *CDKB1;1*; and 5′-AATCTTCAGTTAGTATCTTTCC-AAG-3′ (forward) and 5′-GCTAAAGAAAGGATGATTCATAGAGG-3′ (reverse) for *CDKB2;1*. The threshold cycles at which the fluorescence of the PCR product–SYBR Green complex first exceeded the background level were determined, and the relative template concentration compared with the control was determined based on the standard curve for each gene that was made using a dilution series of cDNA. Relative levels of 18S rRNA were used as a reference. Each PCR was performed in duplicate, and at least three separate biological replicates were measured.

Test for Sensitivity to DNA-Damaging Agents

Seeds were set on agar plates and grown vertically under continuous light for 5 d. To test sensitivity to MMC or MMS, 5-d-old seedlings were transplanted onto the surface of agar plates containing MMC or MMS. The plates were placed vertically so that the new root would grow to the left of the previous root. After a 2-d incubation, root growth was measured and expressed as a percentage of the average length of roots on control plates.

RT-PCR and RNA Gel Blot Hybridization for TSI

RT-PCR for TSI was performed as described (Saze et al., 2003). The specific probe for TSI was a kind gift from J. Paszkowski of the Department of Plant Biology, University of Geneva. RNA gel blot hybridization for TSI was performed as described previously (Steimer et al., 2000).

Assay of Intrachromosomal Recombination

The *teb-1* mutant was crossed with lines F25 and F40 (ecotype Col-0), which carry a reporter construct for intrachromosomal recombination (Urawa et al., 2001). Three-week-old F2 plants carrying this construct were selected by amplification of the GUS gene with PCR and were histochemically stained for GUS activity, as described previously (Urawa et al., 2001).

Accession Numbers

Sequence data from this article can be found in the GenBank/EMBL data libraries under accession numbers AB192295 (*Arabidopsis thaliana* TEB), NP524333 (*Drosophila melanogaster* MUS308), NP084253 (*Mus musculus* POLQ), and NP006587 (*Homo sapiens* POLQ).

Supplemental Data

The following materials are available in the online version of this article.

Supplemental Figure 1. Mapping of the *teb* Mutation.

Supplemental Figure 2. Allelism Test between *teb-1* and T-DNA Insertion Lines.

Supplemental Table 1. Markers Used in Mapping of the *teb* Mutation.

REFERENCES

Abraham, R.T. (2001). Cell cycle checkpoint signaling through the ATM and ATR kinases. Genes Dev. **15,** 2177–2196.

Alonso, J.M., et al. (2003). Genome-wide insertional mutagenesis of *Arabidopsis thaliana.* Science **301,** 653–657.

Barbour, L., and Xiao, W. (2003). Regulation of alternative replication bypass pathways at stalled replication forks and its effects on genome stability: A yeast model. Mutat. Res. **532,** 137–155.

Bilbao, C., Ferreiro, J.A., Comendador, M.A., and Sierra, L.M. (2002). Influence of *mus201* and *mus308* mutations of *Drosophila mela-nogaster* on the genotoxicity of model chemicals in somatic cells in vivo measured with the comet assay. Mutat. Res. **503,** 11–19.

Birnbaum, K., Shasha, D.E., Wang, J.Y., Jung, J.W., Lambert, G.M., Galbraith, D.W., and Benfey, P.N. (2003). A gene expression map of the *Arabidopsis* root. Science **302,** 1956–1960.

Boisnard-Lorig, C., Colon-Carmona, A., Bauch, M., Hodge, S., Doerner, P., Bancharel, E., Dumas, C., Haseloff, J., and Berger, F. (2001). Dynamic analyses of the expression of the HISTONE::YFP fusion protein in Arabidopsis show that syncytial endosperm is divided in mitotic domains. Plant Cell **13,** 495–509.

Boyd, J.B., Sakaguchi, K., and Harris, P.V. (1990). *mus308* mutants of *Drosophila* exhibit hypersensitivity to DNA cross-linking agents and are defective in a deoxyribonuclease. Genetics **125,** 813–819.

Brewer, B.J., and Fangman, W.L. (1987). The localization of replication origins on ARS plasmids in *S. cerevisiae.* Cell **51,** 463–471.

Britt, A.B. (1999). Molecular genetics of DNA repair in higher plants. Trends Plant Sci. **4,** 20–25.

Bundock, P., and Hooykaas, P. (2002). Severe developmental defects, hypersensitivity to DNA-damaging agents, and lengthened telomeres in Arabidopsis *MRE11* mutants. Plant Cell **14,** 2451–2462.

Carles, C.C., Choffnes-Inada, D., Reville, K., Lertpiriyapong, K., and Fletcher, J.C. (2005). *ULTRAPETALA1* encodes a SAND domain putative transcriptional regulator that controls shoot and floral meristem activity in *Arabidopsis.* Development **132,** 897–911.

Clark, S.E., Running, M.P., and Meyerowitz, M. (1995). *CLAVATA3* is a specific regulator of shoot and floral meristem development affecting the same processes as *CLAVATA1.* Development **121,** 2057–2067.

Colon-Carmona, A., You, R., Haimovitch-Gal, T., and Doerner, P. (1999). Technical advance. Spatio-temporal analysis of mitotic activity with a labile cyclin-GUS fusion protein. Plant J. **20,** 503–508.

Costanzo, V., Robertson, K., Bibikova, M., Kim, E., Grieco, D., Gottesman, M., Carroll, D., and Gautier, J. (2001). Mre11 protein complex prevents double-strand break accumulation during chromosomal DNA replication. Mol. Cell **8,** 137–147.

Culligan, K., Tissier, A., and Britt, A. (2004). ATR regulates a G2-phase cell-cycle checkpoint in *Arabidopsis thaliana.* Plant Cell **16,** 1091–1104.

Deveaux, Y., Alonso, B., Pierrugues, O., Godon, C., and Kazmaier, M. (2000). Molecular cloning and developmental expression of *AtGR1*, a new growth-related Arabidopsis gene strongly induced by ionizing radiation. Radiat. Res. **154,** 355–364.

Di Laurenzio, L., Wysocka-Diller, J., Malamy, J.E., Pysh, L., Helariutta, Y., Freshour, G., Hahn, M.G., Feldmann, K.A., and Benfey, P.N. (1996). The *SCARECROW* gene regulates an asymmetric cell division that is essential for generating the radial organization of the Arabidopsis root. Cell **86,** 423–433.

Donnelly, P.M., Bonetta, D., Tsukaya, H., Dengler, R.E., and Dengler, N.G. (1999). Cell cycling and cell enlargement in developing leaves of *Arabidopsis.* Dev. Biol. **215,** 407–419.

Enomoto, S., and Berman, J. (1998). Chromatin assembly factor I contributes to the maintenance, but not the re-establishment, of silencing at the yeast silent mating loci. Genes Dev. **12,** 219–232.

Fletcher, J.C. (2001). The *ULTRAPETALA* gene controls shoot and floral meristem size in *Arabidopsis.* Development **128,** 1323–1333.

Fukaki, H., Wysocka-Diller, J., Kato, T., Fujisawa, H., Benfey, P.N., and Tasaka, M. (1998). Genetic evidence that the endodermis is essential for shoot gravitropism in *Arabidopsis thaliana.* Plant J. **14,** 425–430.

Garcia, V., Bruchet, H., Camescasse, D., Granier, F., Bouchez, D., and Tissier, A. (2003). *AtATM* is essential for meiosis and the somatic response to DNA damage in plants. Plant Cell **15,** 119–132.

Green, K.A., Prigge, M.J., Katzman, R.B., and Clark, S.E. (2005). CORONA, a member of the class III homeodomain leucine zipper gene family in Arabidopsis, regulates stem cell specification and organogenesis. Plant Cell **17,** 691–704.

Guyomarc'h, S., Vernoux, T., Traas, J., Zhou, D.X., and Delarue, M. (2004). *MGOUN3*, an *Arabidopsis* gene with tetratricopeptide-repeat-related motifs, regulates meristem cellular organization. J. Exp. Bot. **55,** 673–684.

Harris, P.V., Mazina, O.M., Leonhardt, E.A., Case, R.B., Boyd, J.B., and Burtis, K.C. (1996). Molecular cloning of *Drosophila mus308*, a gene involved in DNA cross-link repair with homology to prokaryotic DNA polymerase I genes. Mol. Cell. Biol. **16,** 5764–5771.

Helariutta, Y., Fukaki, H., Wysocka-Diller, J., Nakajima, K., Jung, J., Sena, G., Hauser, M.T., and Benfey, P.N. (2000). The *SHORT-ROOT* gene controls radial patterning of the *Arabidopsis* root through radial signaling. Cell **101,** 555–567.

Jenik, P.D., Jurkuta, R.E., and Barton, M.K. (2005). Interactions between the cell cycle and embryonic patterning in *Arabidopsis* uncovered by a mutation in DNA polymerase ε. Plant Cell **17,** 3362–3377.

Jurgens, G., and Mayer, U. (1994). Arabidopsis. In A Color Atlas of Developing Embryos, J. Bard, ed (London: Wolfe Publishing), pp. 7–21.

Kaya, H., Shibahara, K.I., Taoka, K.I., Iwabuchi, M., Stillman, B., and Araki, T. (2001). *FASCIATA* genes for chromatin assembly factor-1 in *Arabidopsis* maintain the cellular organization of apical meristems. Cell **104,** 131–142.

Keil, R.L., and Roeder, G.S. (1984). Cis-acting, recombination-stimulating activity in a fragment of the ribosomal DNA of *S. cerevisiae.* Cell **39,** 377–386.

Klimyuk, V.I., and Jones, J.D. (1997). *AtDMC1*, the *Arabidopsis* homologue of the yeast *DMC1* gene: Characterization, transposon-induced allelic variation and meiosis-associated expression. Plant J. **11,** 1–14.

Kobayashi, T., Hidaka, M., Nishizawa, M., and Horiuchi, T. (1992). Identification of a site required for DNA replication fork blocking activity in the rRNA gene cluster in *Saccharomyces cerevisiae.* Mol. Gen. Genet. **233,** 355–362.

Lafarge, S., and Montane, M.H. (2003). Characterization of *Arabidopsis thaliana* ortholog of the human breast cancer susceptibility gene 1: *AtBRCA1*, strongly induced by gamma rays. Nucleic Acids Res. **31,** 1148–1155.

Laufs, P., Dockx, J., Kronenberger, J., and Traas, J. (1998). *MGOUN1* and *MGOUN2*: Two genes required for primordium initiation at the shoot apical and floral meristems in *Arabidopsis thaliana.* Development **125,** 1253–1260.

Laux, T., Mayer, K.F., Berger, J., and Jurgens, G. (1996). The *WUSCHEL* gene is required for shoot and floral meristem integrity in *Arabidopsis.* Development **122,** 87–96.

Leonhardt, E.A., Henderson, D.S., Rinehart, J.E., and Boyd, J.B. (1993). Characterization of the *mus308* gene in *Drosophila melanogaster.* Genetics **133,** 87–96.

Leyser, H.M.O., and Furner, I.J. (1992). Characterisation of three shoot apical meristem mutants of *Arabidopsis thaliana.* Development **116,** 397–403.

Lupo, R., Breiling, A., Bianchi, M.E., and Orlando, V. (2001). *Drosophila* chromosome condensation proteins Topoisomerase II and Barren colocalize with Polycomb and maintain *Fab-7* PRE silencing. Mol. Cell **7,** 127–136.

Marini, F., Kim, N., Schuffert, A., and Wood, R.D. (2003). POLN, a nuclear PolA family DNA polymerase homologous to the DNA cross-link sensitivity protein Mus308. J. Biol. Chem. **278,** 32014–32019.

Mayer, K.F., Schoof, H., Haecker, A., Lenhard, M., Jurgens, G., and Laux, T. (1998). Role of *WUSCHEL* in regulating stem cell fate in the *Arabidopsis* shoot meristem. Cell **95,** 805–815.

Menges, M., Hennig, L., Gruissem, W., and Murray, J.A. (2002). Cell cycle-regulated gene expression in *Arabidopsis.* J. Biol. Chem. **277,** 41987–42002.

Monson, E.K., de Bruin, D., and Zakian, V.A. (1997). The yeast Cac1 protein is required for the stable inheritance of transcriptionally repressed chromatin at telomeres. Proc. Natl. Acad. Sci. USA **94,** 13081–13086.

Murashige, T., and Skoog, F. (1962). A revised medium for growth and bioassays with tobacco cell cultures. Physiol. Plant. **15,** 473–497.

Nakajima, K., Sena, G., Nawy, T., and Benfey, P.N. (2001). Intercellular movement of the putative transcription factor SHR in root patterning. Nature **413,** 307–311.

Oshige, M., Aoyagi, N., Harris, P.V., Burtis, K.C., and Sakaguchi, K. (1999). A new DNA polymerase species from *Drosophila melanogaster*: A probable *mus308* gene product. Mutat. Res. **433,** 183–192.

Prigge, M.J., Otsuga, D., Alonso, J.M., Ecker, J.R., Drews, G.N., and Clark, S.E. (2005). Class III homeodomain-leucine zipper gene family members have overlapping, antagonistic, and distinct roles in Arabidopsis development. Plant Cell **17,** 61–76.

Sabatini, S., Beis, D., Wolkenfelt, H., Murfett, J., Guilfoyle, T., Malamy, J., Benfey, P., Leyser, O., Bechtold, N., Weisbeek, P., and Scheres, B. (1999). An auxin-dependent distal organizer of pattern and polarity in the *Arabidopsis* root. Cell **99,** 463–472.

Saze, H., Scheid, O.M., and Paszkowski, J. (2003). Maintenance of CpG methylation is essential for epigenetic inheritance during plant gametogenesis. Nat. Genet. **34,** 65–69.

Scheres, B., Laurenzio, L.D., Willemsen, V., Hauser, M.T., Janmaat, K., Wisbeek, P., and Benfey, P.N. (1995). Mutations affecting the

radial organization of the *Arabidopsis* root display specific defects throughout the embryonic axis. Development **121**, 53–62.

Scheres, B., Wolkenfelt, H., Willemsen, V., Terlouw, M., Lawson, E., Dean, C., and Weisbeek, P. (1994). Embryonic origin of the *Arabidopsis* primary root and root meristem initials. Development **120**, 2475–2487.

Schoof, H., Lenhard, M., Haecker, A., Mayer, K.F., Jurgens, G., and Laux, T. (2000). The stem cell population of *Arabidopsis* shoot meristems is maintained by a regulatory loop between the *CLAVATA* and *WUSCHEL* genes. Cell **100**, 635–644.

Segers, G., Gadisseur, I., Bergounioux, C., de Almeida Engler, J., Jacqmard, A., Van Montagu, M., and Inze, D. (1996). The *Arabidopsis* cyclin-dependent kinase gene *cdc2bAt* is preferentially expressed during S and G2 phases of the cell cycle. Plant J. **10**, 601–612.

Seki, M., Marini, F., and Wood, R.D. (2003). POLQ (Pol θ), a DNA polymerase and DNA-dependent ATPase in human cells. Nucleic Acids Res. **31**, 6117–6126.

Shiloh, Y. (2003). ATM and related protein kinases: Safeguarding genome integrity. Nat. Rev. Cancer **3**, 155–168.

Shima, N., Hartford, S.A., Duffy, T., Wilson, L.A., Schimenti, K.J., and Schimenti, J.C. (2003). Phenotype-based identification of mouse chromosome instability mutants. Genetics **163**, 1031–1040.

Siddiqui, N.U., Stronghill, P.E., Dengler, R.E., Hasenkampf, C.A., and Riggs, C.D. (2003). Mutations in *Arabidopsis* condensin genes disrupt embryogenesis, meristem organization and segregation of homologous chromosomes during meiosis. Development **130**, 3283–3295.

Smith, S., and Stillman, B. (1989). Purification and characterization of CAF-I, a human cell factor required for chromatin assembly during DNA replication in vitro. Cell **58**, 15–25.

Sorrell, D.A., Marchbank, A., McMahon, K., Dickinson, J.R., Rogers, H.J., and Francis, D. (2002). A *WEE1* homologue from *Arabidopsis thaliana*. Planta **215**, 518–522.

Steimer, A., Amedeo, P., Afsar, K., Fransz, P., Scheid, O.M., and Paszkowski, J. (2000). Endogenous targets of transcriptional gene silencing in Arabidopsis. Plant Cell **12**, 1165–1178.

Suzuki, T., Inagaki, S., Nakajima, S., Akashi, T., Ohto, M.A., Kobayashi, M., Seki, M., Shinozaki, K., Kato, T., Tabata, S., Nakamura, K., and Morikami, A. (2004). A novel *Arabidopsis* gene *TONSOKU* is required for proper cell arrangement in root and shoot apical meristems. Plant J. **38**, 673–684.

Suzuki, T., Nakajima, S., Inagaki, S., Hirano-Nakakita, M., Matsuoka, K., Demura, T., Fukuda, H., Morikami, A., and Nakamura, K. (2005a). *TONSOKU* is expressed in S phase of the cell cycle and its defect delays cell cycle progression in *Arabidopsis*. Plant Cell Physiol. **46**, 736–742.

Suzuki, T., Nakajima, S., Morikami, A., and Nakamura, K. (2005b). An *Arabidopsis* protein with a novel calcium-binding repeat sequence interacts with TONSOKU/MGOUN3/BRUSHY1 involved in meristem maintenance. Plant Cell Physiol. **46**, 1452–1461.

Takeda, S., Tadele, Z., Hofmann, I., Probst, A.V., Angelis, K.J., Kaya, H., Araki, T., Mengiste, T., Scheid, O.M., Shibahara, K., Scheel, D., and Paszkowski, J. (2004). *BRU1*, a novel link between responses to DNA damage and epigenetic gene silencing in *Arabidopsis*. Genes Dev. **18**, 782–793.

Tuteja, N., and Tuteja, R. (2004). Unraveling DNA helicases. Motif, structure, mechanism and function. Eur. J. Biochem. **271**, 1849–1863.

Ulmasov, T., Murfett, J., Hagen, G., and Guilfoyle, T.J. (1997). Aux/IAA proteins repress expression of reporter genes containing natural and highly active synthetic auxin response elements. Plant Cell **9**, 1963–1971.

Umeda, M., Umeda-Hara, C., Yamaguchi, M., Hashimoto, J., and Uchimiya, H. (1999). Differential expression of genes for cyclin-dependent protein kinases in rice plants. Plant Physiol. **119**, 31–40.

Urawa, H., Hidaka, M., Ishiguro, S., Okada, K., and Horiuchi, T. (2001). Enhanced homologous recombination caused by the non-transcribed spacer of the rDNA in *Arabidopsis*. Mol. Genet. Genomics **266**, 546–555.

Weigmann, K., and Lehner, C.F. (1995). Cell fate specification by *even-skipped* expression in the *Drosophila* nervous system is coupled to cell cycle progression. Development **121**, 3713–3721.

Williams, L., Grigg, S.P., Xie, M., Christensen, S., and Fletcher, J.C. (2005). Regulation of *Arabidopsis* shoot apical meristem and lateral organ formation by microRNA *miR166g* and its *AtHD-ZIP* target genes. Development **132**, 3657–3668.

Wysocka-Diller, J.W., Helariutta, Y., Fukaki, H., Malamy, J.E., and Benfey, P.N. (2000). Molecular analysis of SCARECROW function reveals a radial patterning mechanism common to root and shoot. Development **127**, 595–603.

Ye, X., Franco, A.A., Santos, H., Nelson, D.M., Kaufman, P.D., and Adams, P.D. (2003). Defective S phase chromatin assembly causes DNA damage, activation of the S phase checkpoint, and S phase arrest. Mol. Cell **11**, 341–351.

Yu, Y., Steinmetz, A., Meyer, D., Brown, S., and Shen, W.H. (2003). The tobacco A-type cyclin, *Nicta;CYCA3;2*, at the nexus of cell division and differentiation. Plant Cell **15**, 2763–2777.

Zhang, Z., Shibahara, K., and Stillman, B. (2000). PCNA connects DNA replication to epigenetic inheritance in yeast. Nature **408**, 221–225.

Zhong, R., and Ye, Z.H. (2004). *amphivasal vascular bundle 1*, a gain-of-function mutation of the *IFL1/REV* gene, is associated with alterations in the polarity of leaves, stems and carpels. Plant Cell Physiol. **45**, 369–385.